Time Variation of 500 mb Height Fluctuations with Long, Intermediate and Short Time Scales as Deduced from Lag-Correlation Statistics[1]

MAURICE L. BLACKMON AND Y.-H. LEE
National Center for Atmospheric Research,[2] Boulder, CO 80307
JOHN M. WALLACE AND HUANG-HSIUNG HSU
Department of Atmospheric Sciences, University of Washington, Seattle, WA 98195

(Manuscript received 25 March 1983, in final form 17 November 1983)

ABSTRACT

The time variation of Northern Hemisphere wintertime 500 mb height fluctuations with short, intermediate and long time scales is investigated, using lag-correlation patterns derived from time-filtered data. Fluctuations with short (2.5–6 day periods) time scales propagate eastward at a rate consistent with the notion of a steering level around 700 mb, which supports an interpretation in terms of baroclinic waves. The mobile teleconnection patterns associated with the intermediate (10–30 day periods) time scales exhibit a pattern of time variation suggestive a Rossby-wave dispersion, with a predominance of southward dispersion from middle latitudes into the tropics. The geographically fixed teleconnection patterns characteristic of the longer time scales do not show a well-defined pattern of time variation, but their horizontal structure resembles that of the fastest growing normal mode associated with barotropic instability of the climatological mean wintertime flow.

1. Introduction

In the companion paper, Blackmon, Lee and Wallace (1984 hereinafter denoted BLW), have shown that short, intermediate and long time scale fluctuations in the Northern Hemisphere wintertime 500 mb height field are characterized by different spatial structures. Fluctuations with periods shorter than a week assume a wavelike form, with east–west oriented ray paths and wavelengths on the order of 4000 km. This wavelike structure is most clearly defined in the vicinity of the time-averaged jet streams. The wind field is highly anisotropic with most of the kinetic energy residing in the meridional wind component. One-point correlation maps associated with intermediate (10–30 day periods) and long (>>30 day periods) time scale fluctuations are characterized by two kinds of spatial structures: 1) mobile, zonally oriented wavetrains within well-defined waveguides originating in the jet entrance regions, which tend to dominate at intermediate time scales; and 2) geographically fixed north-south dipole patterns straddling the jet exit regions in the Atlantic and Pacific sectors, which tend to dominate at the long time scales.

In the present paper we will consider the time variation of the circulation patterns associated with these same three ranges of time scales as revealed by lag-correlation statistics. The short time scale fluctuations are treated in Section 2, and the intermediate and long time scale fluctuations in Sections 3 and 4, respectively. These results concerning the time variation, together with the results presented by BLW concerning the horizontal structure, provide the basis for a discussion of the dynamical interpretation of the fluctuations in the three different ranges of time scales in Section 5. The dataset and the filters used in this study are the same as those described in BLW, except that interannual variability has been removed from the low-pass filtered and unfiltered time series.

2. Short time scale fluctuations

Figure 1 shows the lag-correlation patterns for bandpass (2.5–6 day periods) filtered 500 mb height fluctuations for lags of −3, −2, · · · 2 and 3 days relative to fluctuations at the base grid-point (40°N, 160°W) which lies near the middle of the Pacific storm track as defined by the bandpass "teleconnectivity" map (Fig. 16 of BLW). The simultaneous correlation map shown in the middle panel is identical to that in Fig. 15a of BLW. In the +1 day lag-correlation pattern, the positive center located over the base grid-point in the simultaneous correlation map is shifted eastward about one-quarter wavelength, and the strongest positive correlation is reduced to 0.75. The same center is discernible in the lag-correlation pattern for the other lags. The eastward displacement is consistently equal to about one-quarter cycle per day of lag; hence the

[1] Contribution No. 660, Department of Atmospheric Sciences, University of Washington, Seattle, WA 98195.

[2] The National Center for Atmospheric Research is sponsored by the National Science Foundation.

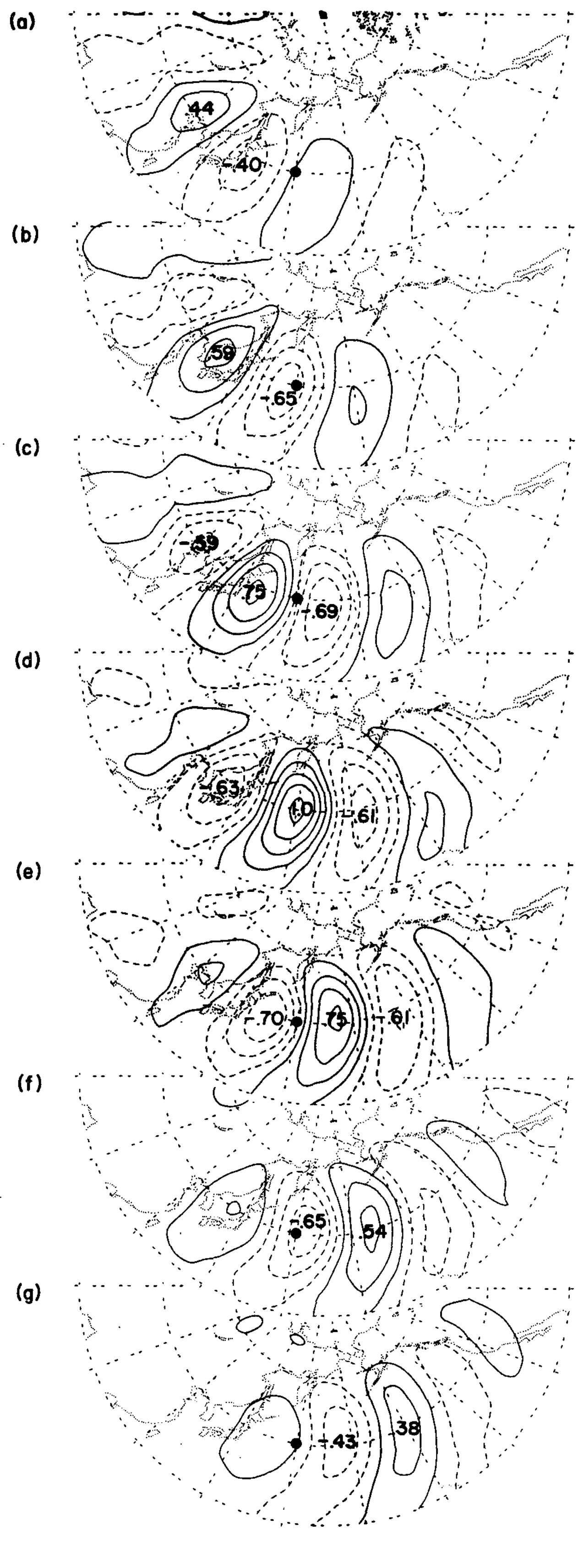

wave progresses eastward with a period of about 4 days, which corresponds to a phase speed of about 15 m s^{-1}. The correlation for the primary positive center located on the base grid point for lag zero drops off by a factor of e in about 3 days for both positive and negative lags.

Figure 2 shows the rate of movement of the band-pass filtered fluctuations for selected grid-points, as inferred from the displacement of the primary positive center during the 2-day interval centered on lag zero. The wind vectors are superimposed upon the 700 mb height field and a few 700 mb geostrophic wind vectors (dashed arrows) are displayed on the chart for the sake of comparison. It is evident that to a rather good approximation the short time scale fluctuations are advected by the 700 mb time mean flow. Similar advection velocities are obtained when one applies the same analysis technique to data filtered with the other band-pass filters described in BLW.

Cahalan *et al.* (1982) reached a similar conclusion based on their analysis of lag-correlation statistics for unfiltered outgoing IR data. The consistency of the results of these two studies suggests that the IR correlation patterns are dominated by fluctuations with periods in the 2.5–6 day band.

3. Intermediate time scale fluctuations

Figures 3–10 show −3 and +3 day lag-correlation maps for low-pass filtered data for selected grid-points. The patterns for the central grid-point of the Eurasian pattern (55°N, 75°E) described by Wallace and Gutzler (1981) are shown in Fig. 3. The corresponding simultaneous correlation pattern appears in Fig. 9 of BLW. It is evident that the time variation of these low-pass filtered fluctuations is much different from that of the band-pass filtered fluctuations in Fig. 1. There is some slight eastward movement of the positive center adjacent to the base grid point in the 6-day interval between Fig. 3a and 3b. However, the dominant form of time variation is the weakening of the upstream centers over the Atlantic and eastern Europe and the strengthening of the downstream centers over the Asian coast and the subtropical western Pacific. Hence, to a first approximation, wave energy disperses along a broad arc extending across Eurasia and southeastward into the Pacific while the phase of the waves remains approximately fixed. Base grid-points located in Eurasia along or near this arc display a similar behavior with respect to their lag-correlation patterns.

FIG. 1. Lag correlation patterns for 500 mb height for the base grid-point (40°N, 160°E) based on band-pass filtered data for lags (relative to the time series at the base grid-point) of −3 days (top panel), −2 days, . . . , +3 days (bottom panel). Contour interval 0.2. Positive contours (0.1, 0.3, etc.) are solid; negative contours (−0.1, −0.3, etc.) are dashed. The heavy dot in each panel denotes the base grid-point.

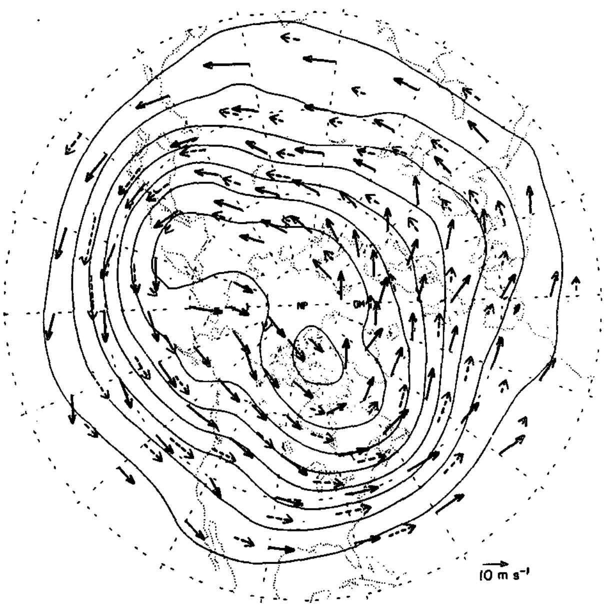

FIG. 2. Solid arrows show phase speed of short time scale fluctuations as inferred from the displacement of the center of the strongest positive correlation between the −1 day and +1 day lag-correlation patterns, divided by 2 days. Dashed arrows show selected velocity vectors for the climatological mean wintertime 700 mb flow. Velocity scale is at the lower right. All arrows are centered on the base grid-point for which calculations were made. Contours show the 700 mb height field; contour interval 60 m.

Fig. 4, which shows the corresponding patterns for the base grid-point (55°N, 115°W), is suggestive of energy dispersion along the ray path associated with the Pacific/North American pattern.

Lag-correlation patterns for grid-points located near the regions of strong low frequency variability in the North Pacific and North Atlantic exhibit a slightly different kind of behavior, as illustrated in Figs. 5–7. The −3 day lag-correlation patterns are rather featureless, with only weak upstream centers, whereas the +3 day lag-correlations show stronger energy dispersion along arcs extending eastward from the base grid-point. Such behavior could be interpreted in two ways: either the wave trains are being generated in the vicinity of the base grid-points, or else the regions around the base grid-points are responding to forcing coming from many different directions rather than from a single, well-defined region upstream as in the previous examples.

Somewhat the opposite behavior is displayed by base grid-points at lower latitudes over the western oceans and adjacent land regions: the −3 day lag-correlation patterns show evidence of wave dispersion from well-defined regions upstream, whereas the +3 day lag-correlations show weaker patterns. Examples for base grid-points over the southeastern United States, the western Atlantic, and the western Pacific are shown in Figs. 8–10, respectively. Note that the weak downstream wave trains in the +3 day lag-correlation patterns in Figs. 8 and 9 are directed along different ray paths than the stronger upstream wave trains in the corresponding −3 day patterns.

The types of time variation illustrated in Figs. 3–10 are representative of base grid-points throughout the hemisphere: eastward energy dispersion through quasi-stationary wave trains is quite generally observed, and the strongest correlations are associated with dis-

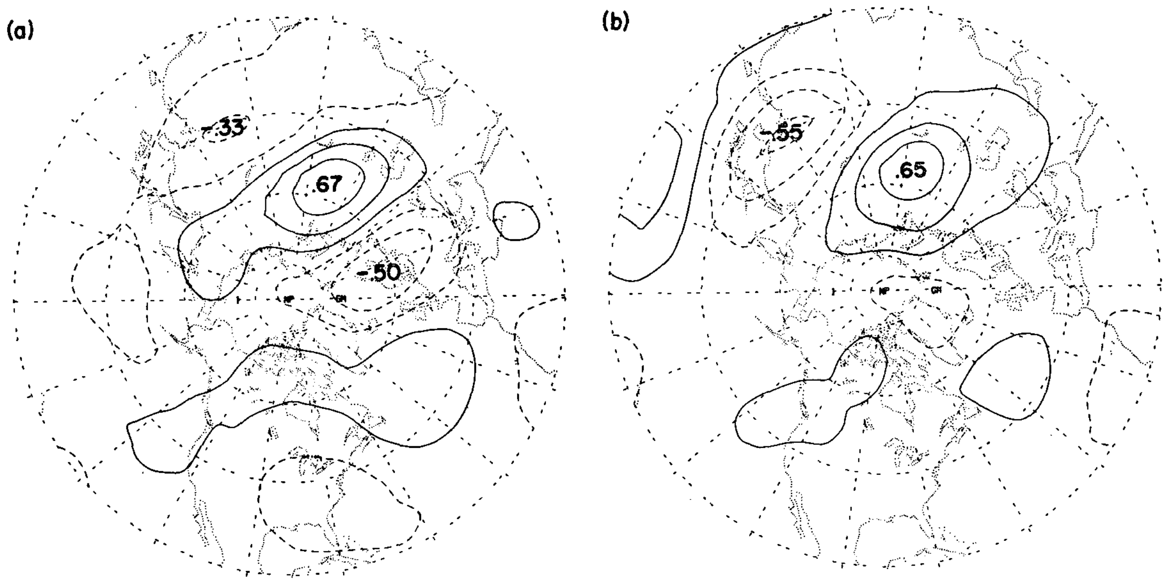

FIG. 3. Lag-correlation patterns for the grid-point (55°N, 75°E) based on low-pass filtered data for lags (relative to the times series at the base grid-point) of −3 days (left) and +3 days (right).

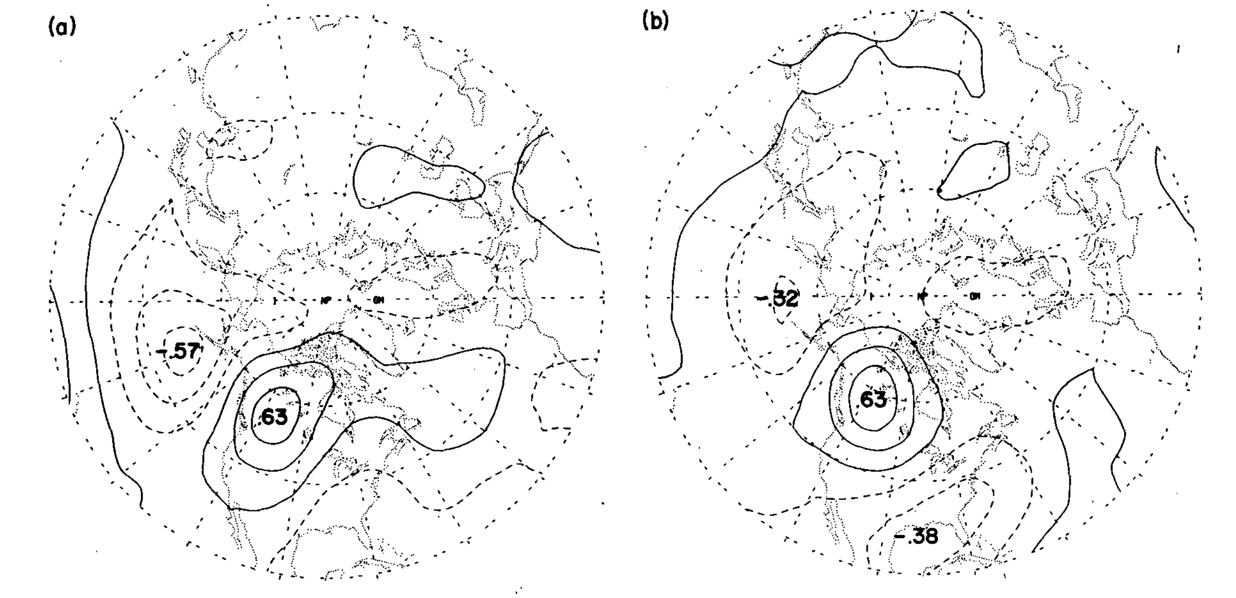

FIG. 4. As in Fig. 3, but for base grid-point (55°N, 115°W).

persion through the three waveguides illustrated in Fig. 13b of BLW.

Figure 11 of this paper shows the composites of 36 lag-correlation patterns computed at 10° longitude intervals along 55, 40 and 25°N, where each pattern is rotated about the North Pole so that the base grid-point is moved to a common reference longitude. These composite patterns are somewhat weaker than the ones for individual grid-points shown previously because the correlation pattern for each individual base grid-point has its own distinctive features. Nevertheless, the energy dispersion phenomenon described here is clearly apparent in these composite patterns. At 40 and 25°N, the energy dispersion is predominantly equatorward as evidenced by the stronger patterns in the −3 day lag-correlation maps and the predominantly northwest/southeast orientation of the wave trains for both negative and positive lags. This result is consistent with

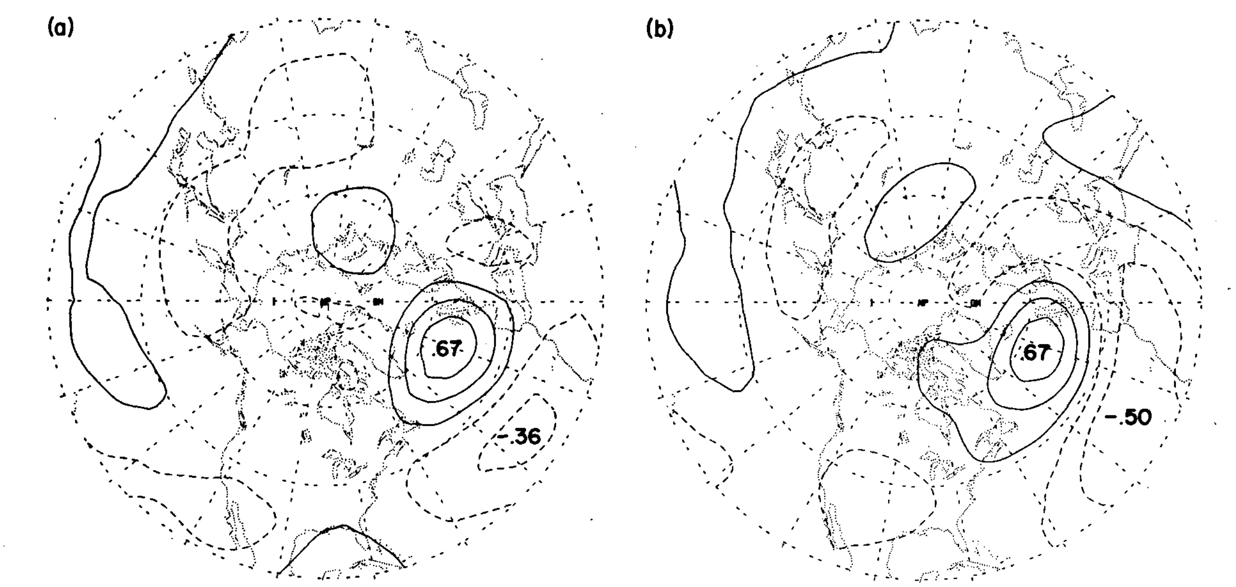

FIG. 5. As in Fig. 3, but for base grid-point (55°N, 20°W).

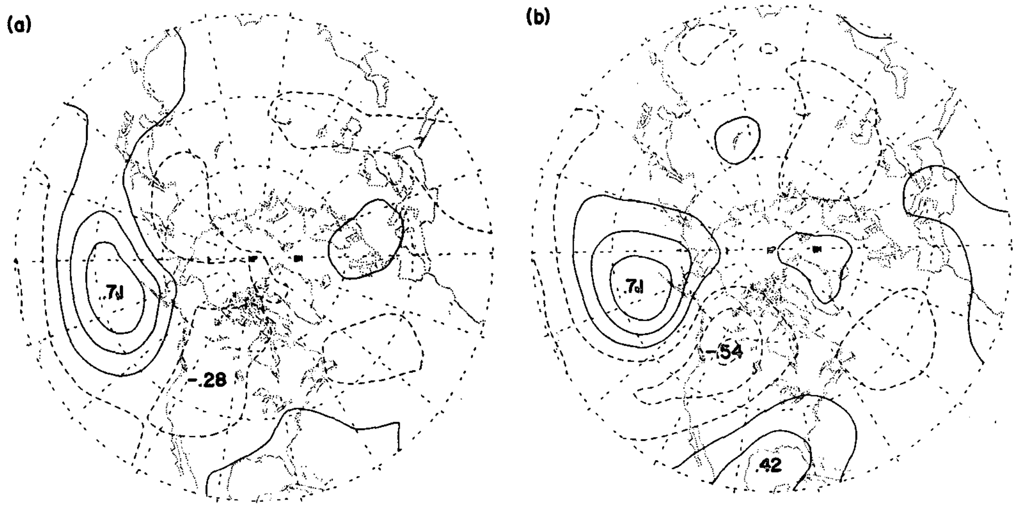

FIG. 6. As in Fig. 3, but for base grid-point (45°N, 165°W).

the predominantly poleward flux of westerly momentum by the low-frequency fluctuations (Blackmon *et al.*, 1977; Lau *et al.*, 1978). At 55°N the energy dispersion is mainly eastward, though there is still some hint of a southward component. Hence it would appear that fluctuations with intermediate time scales are generated predominantly in extratropical latitudes and disperse into the tropics through the preferred waveguides illustrated in Fig. 13b of BLW.

Lag-correlation patterns qualitatively similar to those shown in Figs. 3–10 can be obtained using other filters and for other lag periods. For example, Fig. 12 shows −3 and +3 day lag-correlations for unfiltered data for a base grid-point in the western Atlantic (30°N, 55°W), whose behavior is rather typical. The correlations are weaker than those in the low-pass filtered data (Fig. 9), but the shapes of the patterns appear to be relatively insensitive to the filtering. The corresponding patterns for the −1 and +1 day lag-correlations are shown in Fig. 13. The positive correlations in the vicinity of the base grid-point are higher than those in the previous figure, but the shapes of the patterns are again re-

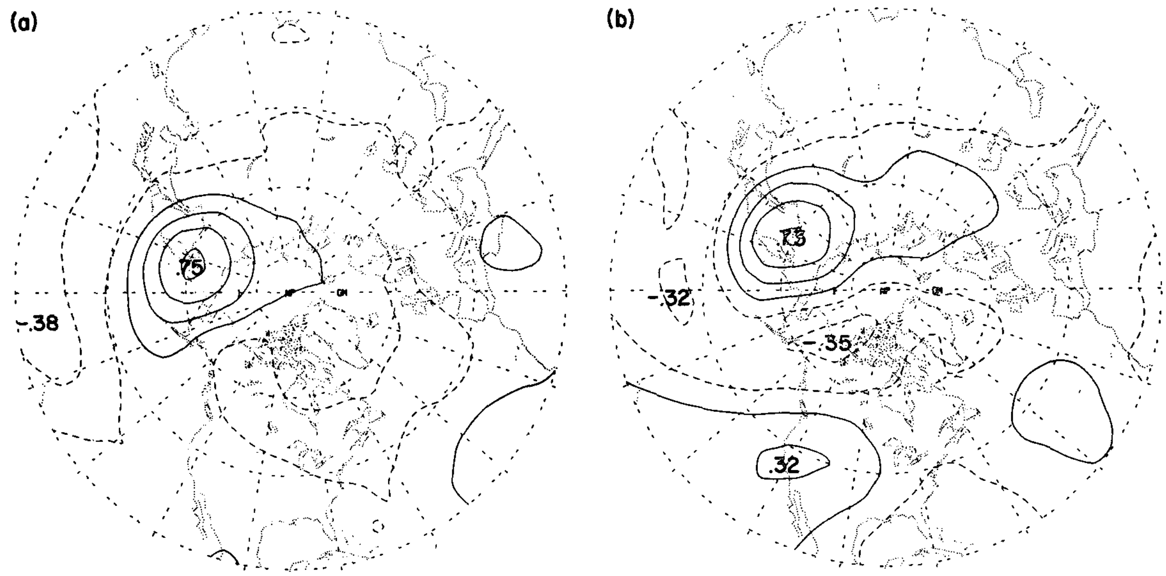

FIG. 7. As in Fig. 3, but for base grid-point (60°N, 155°E).

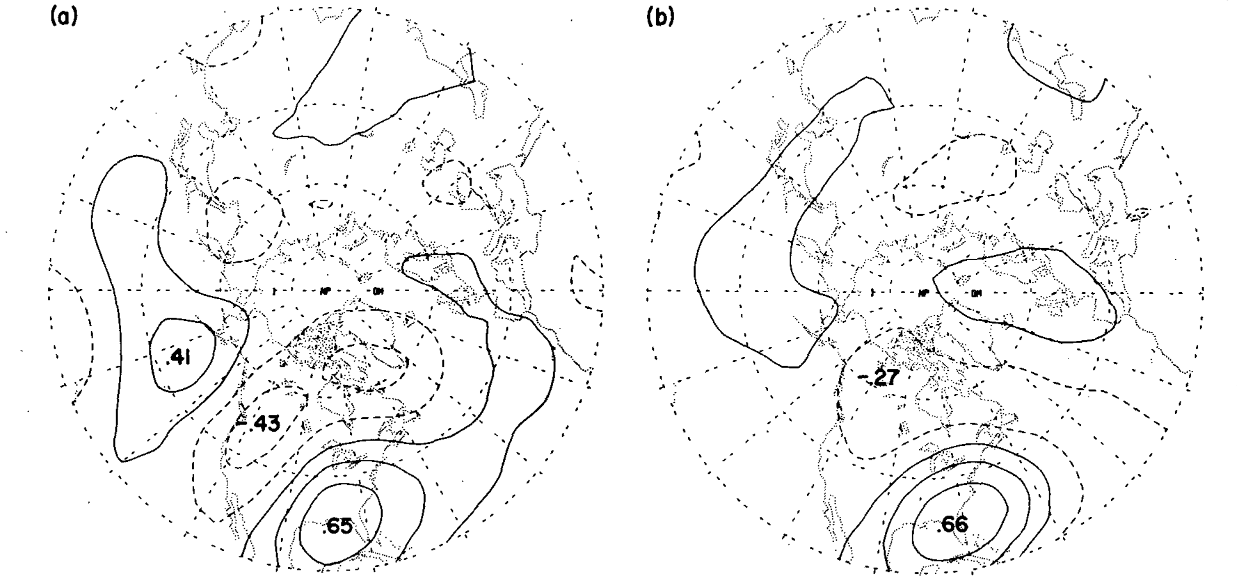

FIG. 8. As in Fig. 3, but for base grid-point (30°N, 85°W).

markably similar to those in Fig. 9. Very similar patterns also appear in the −1 and +1 pentad lag-correlation maps for consecutive, nonoverlapping, 5-day mean data (not shown).

The patterns shown in Figs. 3–10 also resemble the simultaneous correlation patterns for the corresponding grid-points shown in Figs. 4–9 of BLW. It is noteworthy that in all cases the resemblance is strongest for the intermediate time scale fluctuations (10–30 day periods) shown in panel (e) of those figures. This result confirms that it is this intermediate range of time scales which is dominant in the lag-correlation statistics for the unfiltered data and for the low-pass filtered data.

4. Long time scale fluctuations

The time variation of longer period fluctuations can be investigated by applying stronger low-pass filters or time averages to the data and considering longer lag intervals than in the previous section. Fig. 14 shows −10 and +10 day lag-correlations for consecutive 10-

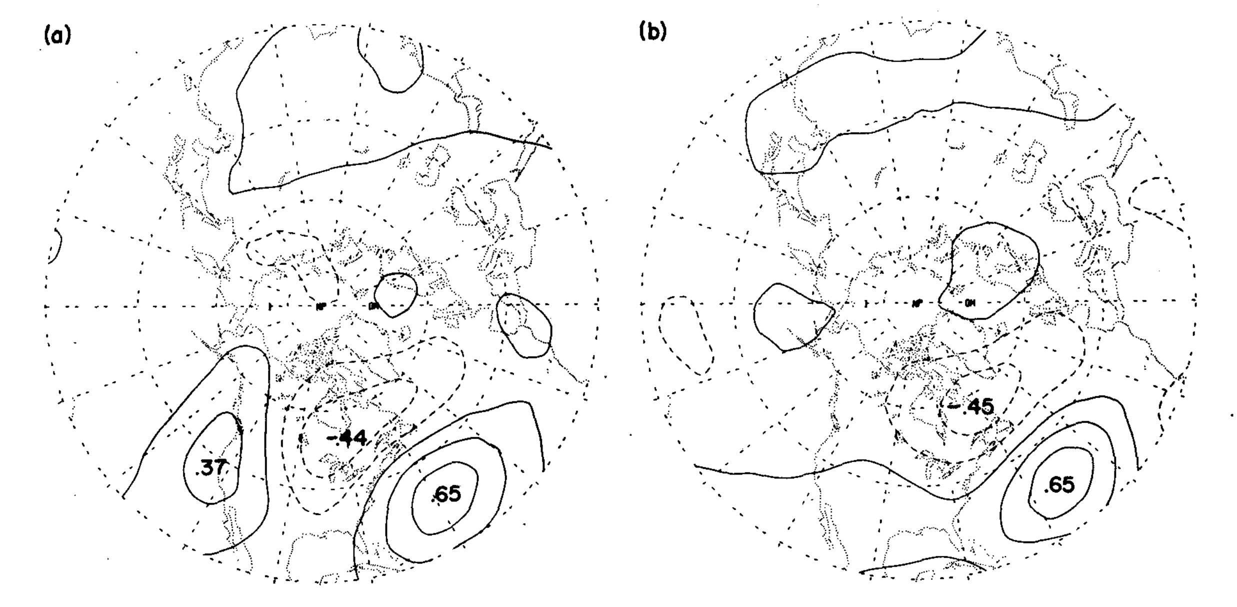

FIG. 9. As in Fig. 3, but for base grid-point (30°N, 55°W).

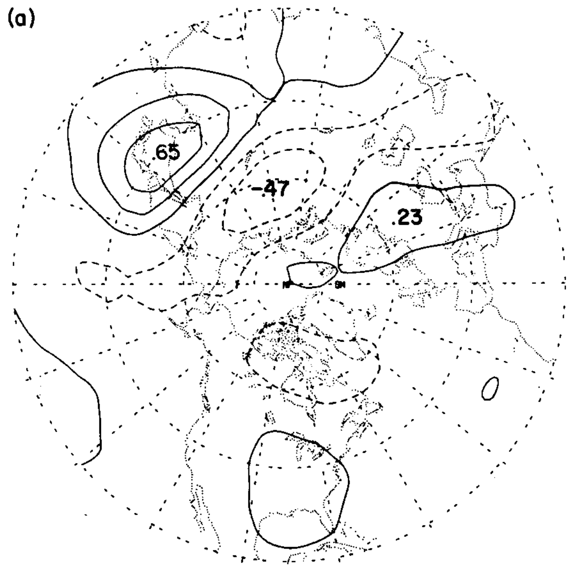

FIG. 10. As in Fig. 3, but for base grid-point (40°N, 140°E).

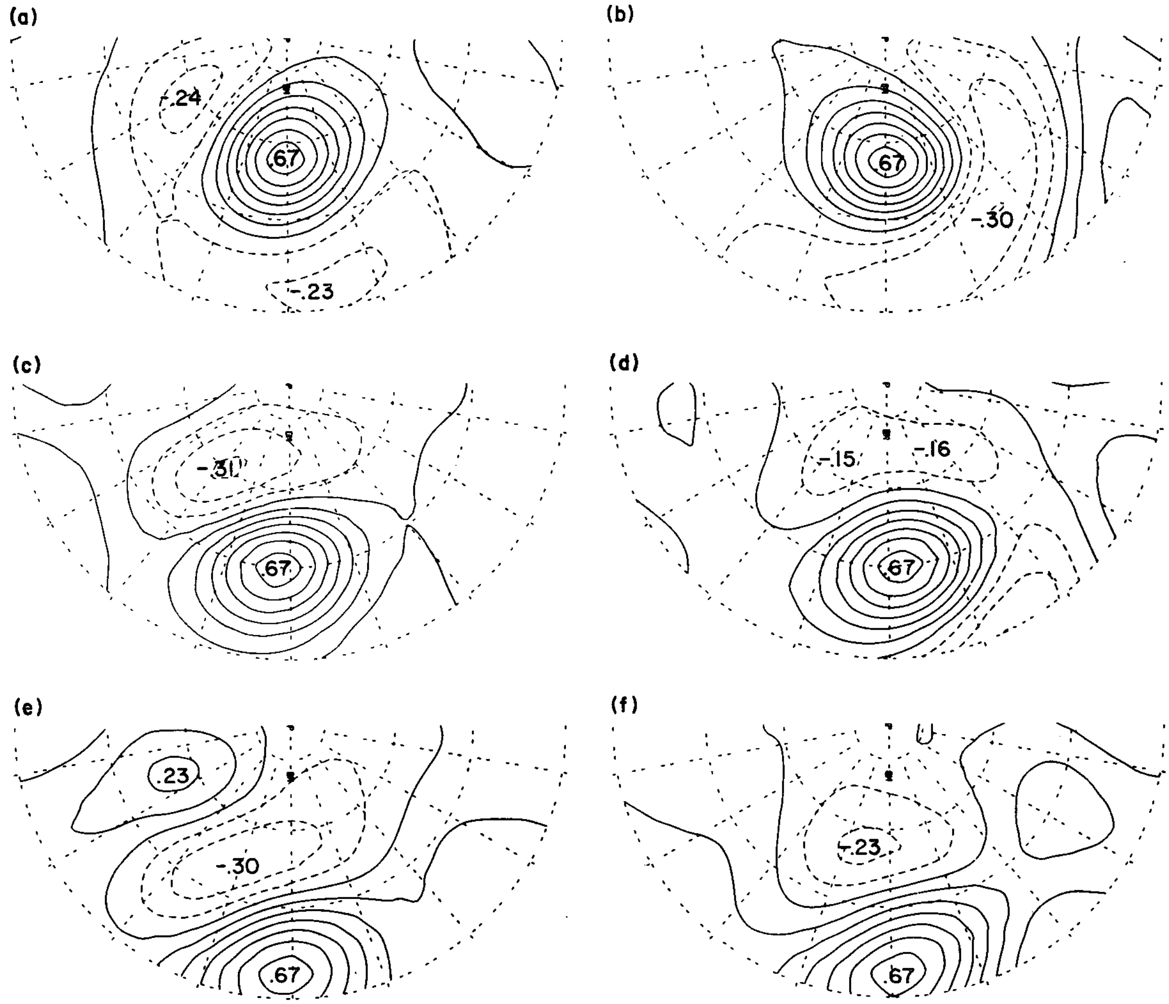

FIG. 11. As in Fig. 3, but for composites of 36 base grid-points located at 10° long intervals along selected latitude circles, with each map rotated about the North Pole so as to bring all base grid-points into coincidence at 0°E. Upper panels, 55°N; middle panels, 40°N; lower panels, 25°N. Lag interval −3 days (left) and +3 days (right).

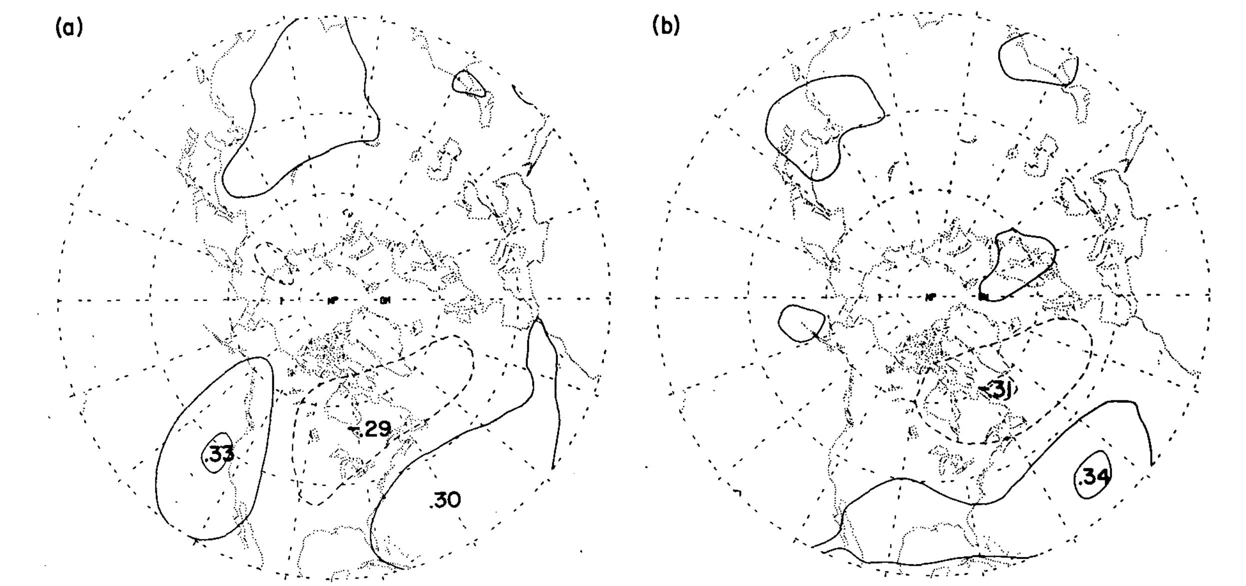

FIG. 12. As in Fig. 9, but for unfiltered daily data for lags (relative to the time series at base grid-point of −3 days (left) and +3 days (right).

day mean data for the same base grid-point as Fig. 9. There is still some hint of the patterns in Fig. 9, but the correlations are weaker and the distinction between the lead- and lag-correlation patterns is much less clear. Further attenuation of the wave dispersion "signal" results when the averaging time and lag interval are extended beyond 10 days. For averaging times of 30 days or longer, the patterns are difficult to distinguish from sampling fluctuations in this 18-winter dataset. Hence it appears that the north–south dipole patterns straddling the jet exit regions, which are dominant in the long time scale fluctuations, do not exhibit any distinctive pattern of time variation of their own.

5. Discussion

The behavior of fluctuations with short time scales, described in BLW and in Section 2 of this paper, is reminiscent of the vivid description of cyclone waves which appeared in a review paper of V. Bjerknes (1920):

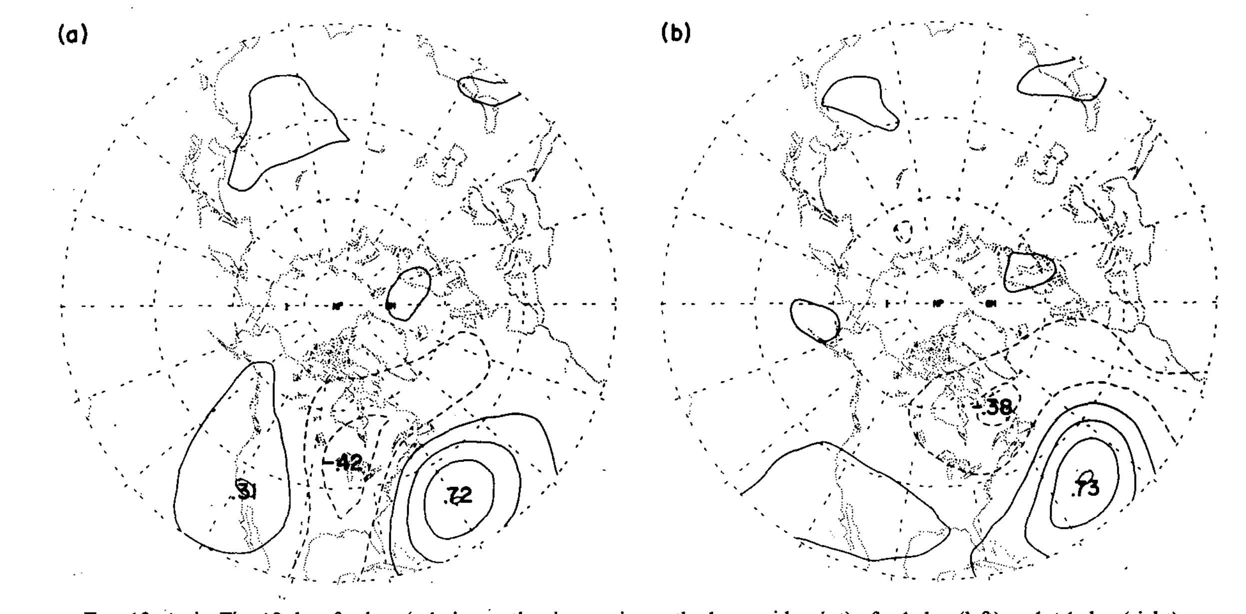

FIG. 13. As in Fig. 13, but for lags (relative to the time series at the base grid-point) of −1 day (left) and +1 day (right).

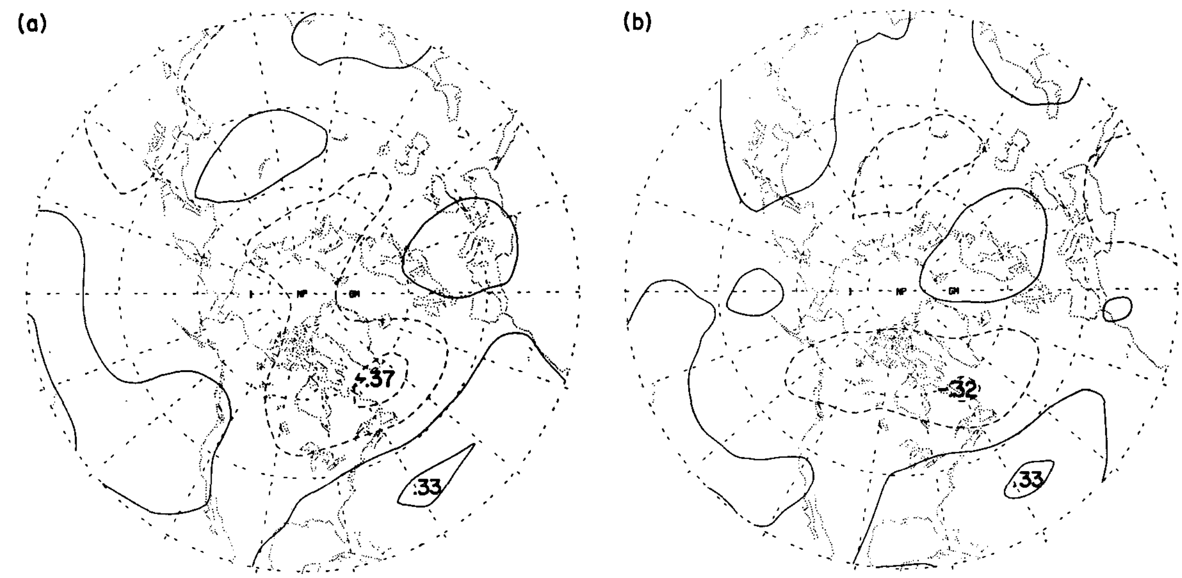

FIG. 14. As in Fig. 9, but for consecutive 10-day mean data for lags (relative to the time series at base grid-point) of −10 days (left) and +10 days (right).

> The cyclones follow each other along a common line of discontinuity, like pearls on a string. . . . The line has a wavy form and is in a continuous undulating motion. . . . The whole system is moving from west to east, while the line, at the same time, changes its form, especially when great masses of accumulated cold air are expelled from the central polar regions.

The earlier literature also contains references to the types of behavior characteristic of fluctuations in the intermediate range of time scales. Willett's (1944) description of the response over North America to the development of an upper level trough over the eastern Pacific resembles the sequence of events that might be observed in connection with energy dispersion through the Pacific/North American pattern. The structure and time variation of such disturbances can be interpreted in terms of the theory of Rossby-wave dispersion on a sphere. (For a recent review of the theoretical literature on this subject see Hoskins, 1983). The characteristic time scales associated with Rossby-wave dispersion are such that, in the absence of any instabilities, the wave train which constitutes the response to a steady, localized forcing, impulsively turned on at time $t = 0$, is fully developed within about a week and thereafter assumes a steady configuration. The filtering procedure employed in Section 3 should be well suited for resolving the time variation associated with this phenomenon which, in our nomenclature, is associated with variability in intermediate time scales. Stronger low-pass filters, such as those employed in Section 4, should not be capable of resolving the development and decay of trains of Rossby-waves. Hence, although the signature of Rossby-wave dispersion is evident, to some extent at least, in the horizontal structure of the long time scale fluctuations, the associated time variation must be governed by other processes.

Nonlinear integration with a barotropic model by Simmons *et al.* (1983) indicate that, in the absence of other influences, the normal mode structures associated with barotropic instability exhibit a well-defined pattern of time variation with characteristic time scales on the order of weeks or months. The absence of well-defined patterns in the lag-correlation statistics for the long time scales, despite the strong signature of the normal modes in the geographically fixed dipole patterns straddling the jet exit regions, suggests that time variability at these long time scales is determined more by the changing distribution of the forcing of the planetary-scale flow than by the internal dynamics of barotropic instability.

Because of their resemblance to the normal modes associated with barotropic instability of the climatological mean flow, it is plausible that the Pacific/North American and Eastern Atlantic patterns are excited by forcing from a wide range of locations. If the preferred regions from which the forcing comes are not well-defined, then it is not surprising that the lag-correlation patterns for negative lags are rather poorly defined for the base grid-points in Figs. 5–7. On the other hand, it seems plausible that the excitation of these normal modes should be accompanied by a strong dispersion of energy toward the downstream centers of action, which would account for the relatively stronger lag-correlation patterns for positive lags.

The strong equatorward energy dispersion in the low-latitude patterns as manifested in stronger patterns for the negative lags and the prevailing northwest–southeast orientation of the patterns, indicate that most of the forcing for the fluctuations in the intermediate

TABLE 1. Characteristics of wintertime 500 mb height fluctuations as a function of time scale.

	Short	Intermediate	Long
Period (days)	2.5–6	10–30	>>30
Predominant zonal wavenumbers	6–9	4–6	1–4
Mode of spatial organization	Storm tracks related to jet streams	Mobile wave trains oriented along waveguides originating in jet entrance regions (BLW, Fig. 13b)	Geographically fixed north-south dipole patterns straddling the jet exit regions (BLW, Fig. 13a)
Mode of time variation	Advection of wave trains by 700 mb steering flow	Dispersion through stationary wave trains	Not well-defined
Theoretical interpretation	Baroclinic waves	Two-dimensional Rossby-wave dispersion	Still unclear; see BLW

time scale range comes from middle latitudes. However, the dominance of equatorward energy dispersion across 30°N does not preclude the possibility that tropical forcing could make an important contribution to the long time scale variability, or that it could, in specific instances, give rise to shorter period fluctuations.

The patterns in Figs. 4 and 5 bear a strong resemblance to Dole's (1982) time composites of low-pass filtered 500 mb height anomalies associated with large, persistent positive and negative anomalies at (45°N, 170°W), which lie close to one of the base grid-points of the Pacific/North American pattern. In both our analysis and in Dole's, the sequence of events preceding the onset of the large anomalies is not very well marked, but the development of the anomalies in the vicinity of the base grid-point is followed, within several days, by the appearance of a wave train downstream over North America. The breakdown of Dole's persistent anomalies at the base grid-point appears to proceed in a similar manner. Dole also examined persistent anomalies in the North Atlantic, and over the Soviet Union at the base grid point (60°N, 60°W). The time variation of these features bears a rather strong relation to our Figs. 7 and 3, respectively. Dole also recognized the possible importance of two dimensional Rossby-wave dispersion in the interpretation of his results. The consistency between Dole's results and our own, despite the fact that the two studies are based on entirely different analysis approaches, enhances the credibility of the results of both studies.

It is also of interest to relate the results presented in the preceding sections to the composite analysis of the cold air outbreaks over East Asia by Joung and Hitchman (1982). On average, these events were found to be preceded by the development of a large amplitude wave pattern over the Eurasian continent with a trough over Scandinavia 3–4 days earlier, a ridge over Siberia near (60°N, 80°E), which reached its maximum amplitude about 2 days before the cold air outbreak, and ultimately by a trough over Korea whose development coincided with the time of the cold air outbreak. Several days later a ridge developed near the dateline with a branch trailing southwestward over the subtropical western Pacific. (These features are most readily discernible in Fig. 4 of their paper.) There is a strong correspondence between the features mentioned above and the lag-correlation patterns shown in Figs. 3 and 10 of the present paper, and Fig. 13b of BLW. However, the Joung and Hitchman composites, which are not filtered in time, are influenced by other aspects of the time variation which are more closely related to the short time scales discussed in Section 2; i.e., most notably, the tendency for individual ridges and troughs to be advected eastward with the time mean flow. The impression conveyed by the superposition of these two distinctly different modes of time variation is that of an eastward phase velocity of the individual ridges and troughs, with a pronounced tendency for downstream development of additional features in the wave train, best exemplified by their Fig. 7. This interpretation does not preclude the possible relevance of the dynamical mechanisms discussed by Joung and Hitchman.

The results of this paper and the companion paper of BLW are outlined in Table 1. This table is not intended as a complete summary of the nature and causes of atmospheric variability as a function of time scale, since it contains no mention of phenomena such as blocking, transitions between multiple equilibrium states and vacillation, which might conceivably contribute to intermediate and long time scale variability. Its sole purpose is to summarize the distinctions between the simultaneous and lag-correlation statistics for short, intermediate, and long time scales.

Acknowledgment. Work for this paper was partially supported under Grant ATM 18-06099, Climate Dynamics Program, National Science Foundation.

REFERENCES

Bjerknes, V., 1920: The meteorology of the temperate zone and the general atmospheric circulation. *Nature,* **105,** 522–524.

Blackmon, M. L., J. M. Wallace, N.-C. Lau and S. L. Mullen, 1977: An observational study of the Northern Hemisphere wintertime circulation. *J. Atmos. Sci.*, **34**, 1040–1053.

——, Y.-H. Lee and J. M. Wallace, 1984: Horizontal structure of 500 mb height fluctuations with long, intermediate and short time scales. *J. Atmos. Sci.*, **41**, 961–979.

Cahalan, R. F., D. A. Short and G. R. North, 1982: Cloud fluctuation statistics. *Mon. Wea. Rev.*, **110**, 26–43.

Dole, R. M., 1982: Persistent anomalies of the Northern Hemisphere wintertime circulation. Ph.D. dissertation, MIT, 225 pp.

Hoskins, B. J., 1983: Dynamical processes in the atmosphere and the use of models. *Quart. J. Roy. Meteor. Soc.*, **109**, 1–21.

Joung, C. H., and M. H. Hitchman, 1982: On the role of successive downstream development in East Asian polar air outbreaks. *Mon. Wea. Rev.*, **110**, 1224–1237.

Lau, N.-C., H. Tennekes and J. M. Wallace, 1978: Maintenance of the momentum flux by transient eddies in the upper troposphere. *J. Atmos. Sci.*, **35**, 139–147.

Simmons, A. J., J. M. Wallace and G. W. Branstator, 1983: Barotropic wave propagation and instability, and atmospheric teleconnection patterns. *J. Atmos. Sci.*, **40**, 1363–1392.

Wallace, J. M., and D. S. Gutzler, 1981: Teleconnections in the geopotential height field during the Northern Hemisphere winter. *Mon. Wea. Rev.*, **109**, 785–812.

Willett, H. C., 1944: *Descriptive Meteorology*. Academic Press, 310 pp.